"AERODYNAMIC PERFORMANCE OF A HIGH-SPEED TURBINE CASCADE WITH AXIALLY CONTOURED ENDWALLS"

[1]Raghu P, [2]Mr R Senthil Kumaran and [3]Dr.K S Shashishekar

[1]*Department of Mechanical Engineering Siddaganga Institute of Technology, Tumakuru, Karnataka, India.*
[2]*Propulsion Division, National Aerospace Laboratory, Bengaluru, Karnataka, India.*
[3]*Department of Mechanical Engineering Siddaganga Institute of Technology, Tumakuru, Karnataka, India.*

Abstract: This paper provides a complete review of the experimental and numerical results demonstrating the aerodynamic performance of a turbine stator cascade. The experimental work involved linear cascade testing in the NAL Transonic Cascade Tunnel (TCT). Used pressure based Navier-Stokes solver of ANSYS CFX for Numerical simulations. The cascade model was tested with two different end wall configurations; straight and contoured converging end walls. By using straight and contoured converging end walls, two different Axial Velocity Density Ratios were simulated. Pitch-wise, wake traverses were carried out across several span locations to map the secondary flow. Experiments were carried out over 0.7 to 1.2 exit Mach numbers at three different angles of incidence including the design condition. Blade loading was measured at three different span locations. Reynolds number close to the actual engine values were simulated during the experiments. Aerodynamic performance parameters like profile loss, flow deflection, blade loading etc., were measured. Oil flow visualization studies were realized to characterize the flow pattern over the blade surfaces and the end walls. Both straight and contoured end wall configurations exhibit similar loss trends at mid span. However, contoured end wall configuration shows fractionally lower pressure loss.

Keywords: AVDR, blade loading, boundary layer, cascade, flow deflection, profile loss, secondary flow, etc.,

NOMENCLATURE

C = Chord of the blade (mm)
βs = Stagger angle (Degree)
β_2 = Outlet flow angle (Degree)
β_2' = Outlet metal angle (Degree)
δ = Deviation angle (Degree)
θ = Blade camber angle (Degree)
λ = Solidity Ratio
k = Turbulent kinetic energy
P_{02} = Exit total pressure (mm of Hg)
p_2 = Outlet static pressure (mm of Hg)
M_2 = Outlet Mach number
y = Pitch wise distance (mm)
HP = High Pressure
TCT = Transonic Cascade Tunnel
C_{ax} = Axial Chord of the blade (mm)
β_1 = Inlet flow angle (Degree)
β_1' = Inlet metal angle (Degree)
i = Incidence angle (Degree)
S = Pitch /Spacing (mm)
ε = Flow deflection (Degree)
μ_t = Turbulent viscosity (Pa s)
P_{01} = Inlet total pressure (mm of Hg)
p_1 = Inlet static pressure (mm of Hg)
M_1 = Inlet Mach number
x = Chord wise distance (mm)
AVDR = Axial Velocity Density Ratio
NGV = Nozzle Guided Vane
SST = Shear Stress Transport turbulence model

1 INTRODUCTION

When the flows are three-dimensional it is very difficult to measure, model & understand. Nowadays the testing of turbine & compressor blades in a cascade is the most common way. A cascade is simply a turbine or compressor that is cut in half along the axis and made to lay down flat. For testing the aerodynamics and other properties more easily the blades are arranged in parallel or in annular way inside the wind tunnel. A wind tunnel is used to find out the effects of fluid flow over the blades. To increase the efficiency of a turbine, need to improve in the turbine section. Very hot gases from combustion chamber enter into gas turbine and expand through the turbine blades, causing it to rotate. The rotation of turbine blade leads to rotate the shaft to provides the power for compressor and in power generation drives an additional generator. High pressure gases exit the turbine and passes through a nozzle at high velocity, creating thrust is required for the propulsion purposes. Pressure drops across each blade cause the rotation.

Due to secondary flows additional pressure losses are created. Grant Laidlaw Ingram [7] emphasized that end-wall profile targets to reduce the unacceptable secondary flow elements by modeling the end-wall in the middle of the turbine blades. The modeling too accelerates the flow which reduces the local static pressure. By using boundary layer fence with a turbine cascade effectually minimizes the strength of the major loss leading to minor aerodynamic losses in the turbine path. So, the total pressure losses within the boundary layer is reduced. By 15% to 25% the total pressure loss is reduced for the fence's heights of 12 mm and 16 mm respectively according to M. Govardhan and P.K. Maharia [6]. The change was obtained in lift and drag coefficients due to reduction in the total pressure loss. Overall, it was concluded the secondary loss can be reduced by fences and increases the performance of the turbine cascade. The profile losses can be reduced by using different end-wall in cascade testing.

II. DESIGN PROCEDURE

A. Profile Details

The turbine stator aerofoil has been designed for a solidity ratio [C / S] of 1.42. The cascade geometry and design flow conditions are listed in Table 1. All angles are in axial direction. At flow condition M_2=0.98 and β_1=0^0.

Table-I: Turbine stator cascade geometry

Parameters	Notation	Magnitude
Stagger angle	β_s	53.50^0
Solidity ratio	λ	1.42
Inlet metal angle	β_1 '	0.0^0
Outlet metal angle	β_2 '	71^0
No. of blades in assembly	N	7

B. Cascade Geometry

The below figure shows the cascade geometry of turbine stator blade profile.

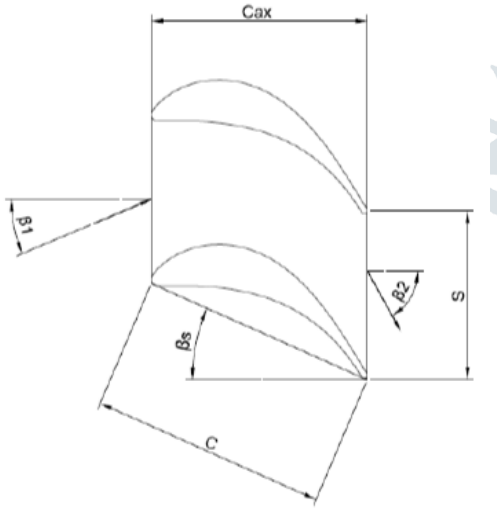

Fig. 1 Cascade geometry.

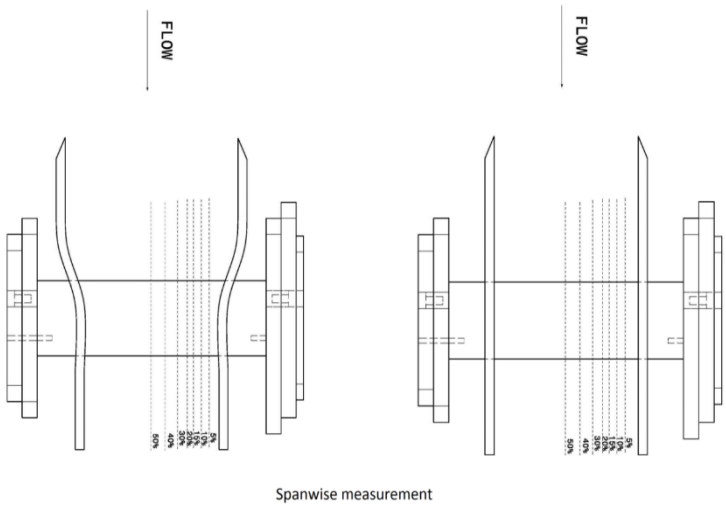

Fig. 2 Wake measurement positions for the cascade.

C. Cascade Model

Secondary flow measurement was carried out for the cascade with both the end wall configurations. Secondary flow was mapped by measuring Wake flow at several span wise locations like 5, 10, 15, 20, 25, 30, 40 and 50%. A five-hole cone probe was traversed at fine pitch-wise interval of 1.5 mm at all the above-mentioned span locations. Secondary flow measurement was made with cascade configurations at the design flow condition of β_1 = 0° and M_2 = 0.98.

D. Arrangement of Blades on Cascade

The blades were mounted at the required pitch and stagger angle on the perspex sheets using the stem and pin arrangement. The stem is used for fixing the pitch and pin is used for setting the stagger angle. Cascade width of 153 mm was maintained and the extra length of the long / instrumented blades was fully embedded on one side of the perspex sheet to facilitate easy access of the instrumentation tubes is shown in figure 2.

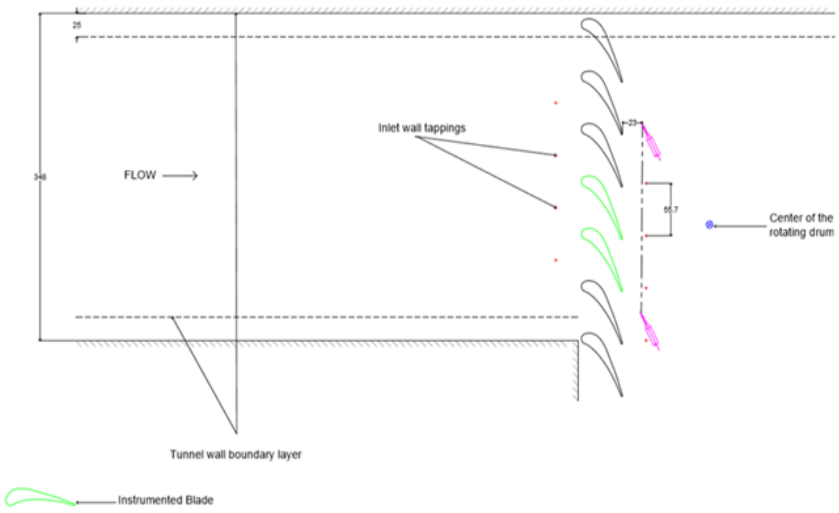

Fig. 3 Schematic view of stator cascade in TCT at 0^0 angle of incidence.

E. Mesh / Grid Generation

The 3D CAD model created in CATIA was saved as an IGES file and imported into the preprocessing tool ICEM for meshing. A hybrid mesh was created for discretizing the control volume. A structured quadrilateral type grid was used near the blade to represent the boundary layer effects. The figure 4 and 5 shows the meshing.

The details of boundary layer mesh
First row thickness: 0.002 mm
Growth Factor: 1.2
Number of lines in the boundary Layer: 30

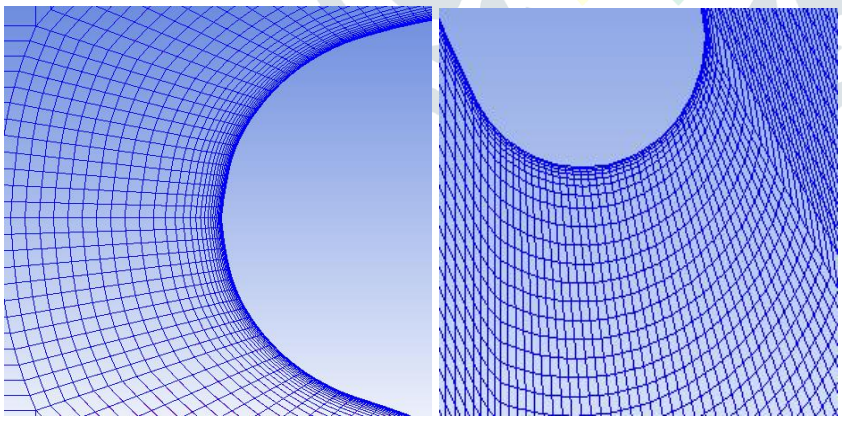

Fig. 4 Meshing near the leading edge and trailing edge.

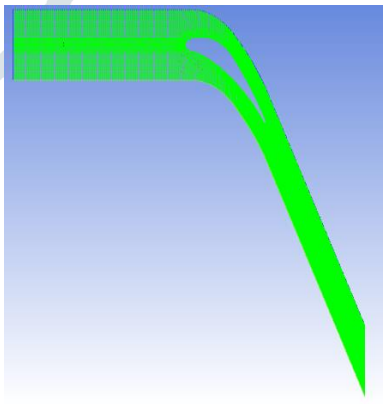

Fig. 5 Fully meshed CFD domain.

F. Grid Independence Study

Grid independence study is taken for minimize the grid size for a model, getting the best accuracy to the solution with the minimum computational time. The simulation must give exact result as number of grid points increases and there should not be considerable alteration on the result with further resizing of the grid.

In both the cases medium sized mesh was used for further simulations, because in the three type of meshes there is no changes in outlet Mach number and total outlet pressure as shown in above tables and for medium mesh data will be converging at less time.

Table-II: Grid independence for different end-wall

End-wall	Mesh	No. of nodes	No. of elements	M_1	M_2
Straight	Medium	511440	482196	0.190	0.982
Contour	Medium	533560	508759	0.1473	0.981

III. CASCADE TEST EXPERIMENTS

A. Transonic Cascade Tunnel

Transonic Cascade Tunnel (TCT) is a high-speed wind tunnel equipped to test linear cascade models of turbine and compressor blade profiles. It uses working fluid as compressed air. For any type of axial flow compressor, gas and steam turbine blade profiles are tested in TCT. It is a blow down tunnel with a test section size of 153*500 mm for testing turbo machinery cascades at transonic/supersonic outlet Mach numbers. It is ideally suited to obtaining blade profile design / performance data in the transonic Mach number range encountered at the final stages of large steam turbines, which use special blade profiles for supersonic flows. The TCT can also cater for quasi-3D studies with coolant flows, end wall secondary flows, inlet boundary layers, inlet turbulence etc. This facility has been extensively used as an imperative tool to accomplish several national and international research programs in the field of turbo machinery. Gostelow in Reference [1].

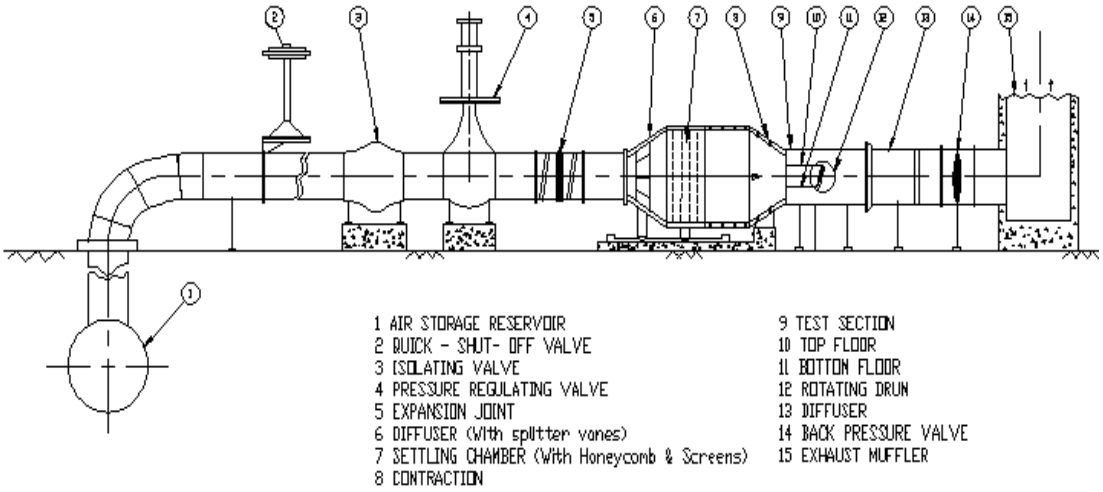

Fig. 6 Schematic layout of the Transonic Cascade Tunnel (TCT).

B. Blade Loading /Pressure Distribution Measurements

The surface pressure distribution is measured by taking number of pressures at the blade surface through hypodermic needles embedded in the blade itself. Two blades are instrumented, one at the suction and the other at pressure side to get the blade channel pressure distribution. All the tubes are drawn inside the blade and taken out through the sidewalls so that these tubes do not disturb the flow. These pressure tubes are connected to multiport pressure measurement device and the readings are acquired through the PC using a data acquisition card for further study.

C. Data Reduction

The responses obtained from the transducers were in the form of millivolts. These data were later converted into engineering units using the calibration data of the transducers. The data measured using the five-hole edge probe was reduced using the probe calibration coefficients. The downstream mixed out or homogenous values were calculated from the local values using a 2D mass averaging technique.

The inlet Mach number calculated by utilizing inlet total and static pressures

$$\frac{P_{01}}{P_1} = \left\{1 + \frac{(\gamma-1)}{2} M_1^2\right\}^{\frac{(\gamma-1)}{\gamma}} \qquad (1)$$

The exit Mach number calculated by utilizing the momentum averaged total and static pressures measured by probe in the wake

$$\frac{P_{02}}{P_2} = \left\{1 + \frac{(\gamma-1)}{2} M_2^{\,2}\right\}^{\frac{(\gamma-1)}{\gamma}} \qquad (2)$$

The pressure loss coefficient 'ξ' is calculated using the following expression

$$\xi = \frac{(P_{02}-P_{01})}{P_{02}-p_2} \qquad (3)$$

IV. RESULTS AND DISCUSSION

The local values can be measured in the wake flow through the five-hole probe are averaged by a two-dimensional momentum method. The data obtained from numerical simulations of the turbine cascade with straight end wall in table III and contoured end wall in IV table.

Table-III: CFD results for straight end-wall configuration.

Run no.	M_1	M_2	Pressure Loss coefficient [$dP_0/(P_{02}-p2)$]	P_{01} mm of Hg	p1 mm of Hg	P_{02} mm of Hg	p2 mm of Hg
33	0.162	0.601	0.062	892.70	876.51	880.58	685.00
21	0.171	0.681	0.063	953.10	933.78	937.40	687.00
34	0.183	0.827	0.065	1104.20	1078.60	1078.95	688.51
35	0.187	0.911	0.077	1218.10	1188.75	1185.14	692.05
36	0.19	1.013	0.090	1469.00	1432.40	1412.5	734.52
37	0.191	1.082	0.094	1664.60	1622.77	1591.43	760.76
38	0.191	1.201	0.100	1863.00	1816.02	1758.46	722.87

Table-IV: CFD results for contoured end-wall configuration.

Run no.	M_1	M_2	Pressure Loss coefficient [$dP_0/(P_{02}-p2)$]	P_{01} mm of Hg	p1 mm of Hg	P_{02} mm of Hg	p2 mm of Hg
88	0.123	0.575	0.067	872.00	862.86	860.32	687.00
86	0.138	0.727	0.069	1004.30	991.10	984.15	692.00
87	0.143	0.818	0.071	1109.60	1093.93	1082.17	696.00
92	0.145	0.901	0.078	1226.00	1208.07	1189.50	701.00
91	0.147	0.998	0.085	1466.00	1444.00	1405.5	742.40
90	0.147	1.094	0.096	1664.00	1639.00	1583.60	745.50
88	0.123	1.575	0.104	872.00	862.86	860.32	687.00

A. Surface Mach Number Distribution at Design Mach Number for 50% Span

The surface Mach number distribution for straight end wall and contoured end wall cases was shown in figure 10. In both cases, the contour end wall having lower peak Mach number than straight end wall at the shock location so, thus reduces the intensity of the shock wave in contour end wall.

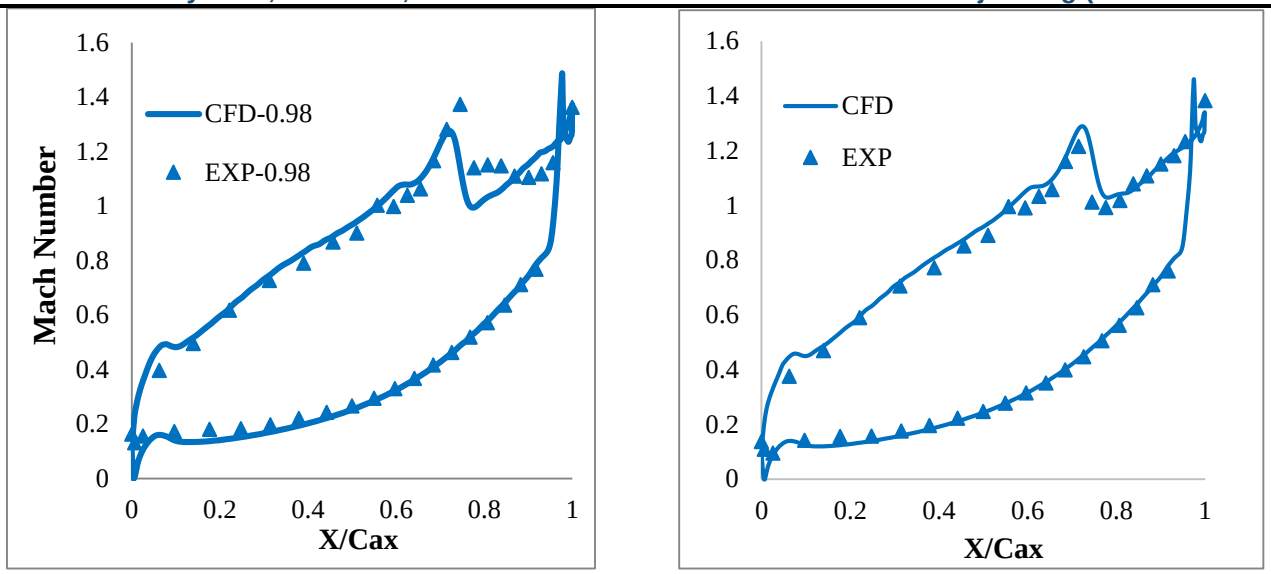

For straight end-wall For Contoured end-wall

Fig. 7 Effect of surface Mach number distribution at design incidence.

B. Effect of Total pressure ratio at design flow condition

The local values of CFD data and experimental data are compared, here the total pressure ratio and outlet Mach number of typical wakes caused by the stator cascade at single pitch is shown below figure. Below data shows good flow periodicity and repeatability across the pitches.

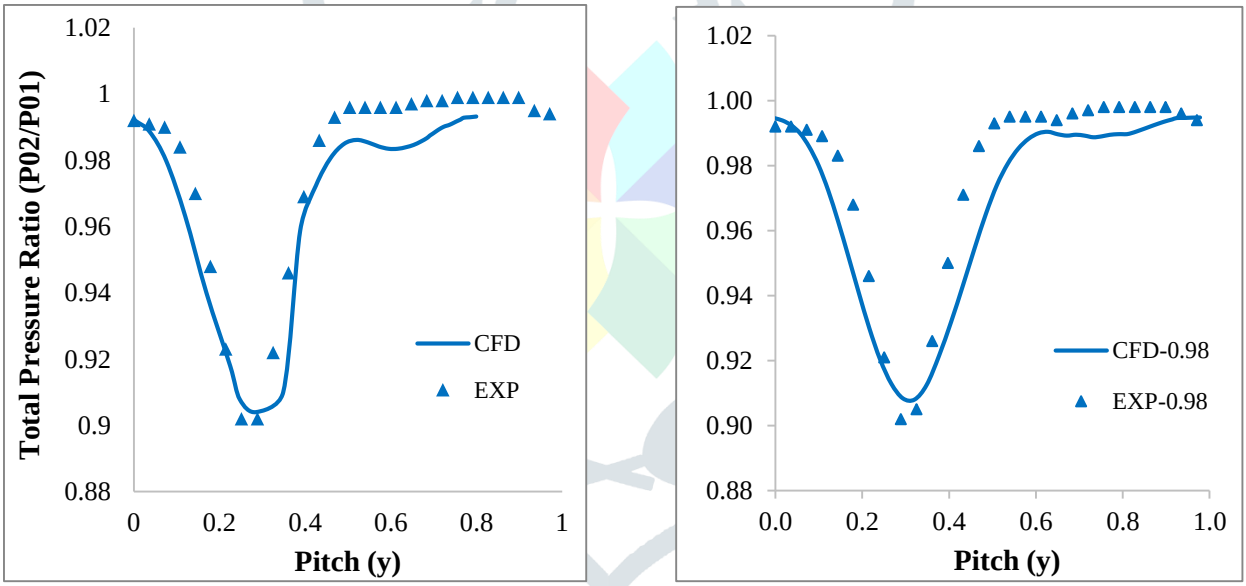

For straight end-wall For Contoured end-wall

Fig. 8 Effect of Total pressure ratio at design incidence.

C. Effect of Incidence on Pressure

The difference in profile loss coefficient along the incidence of an angle 10^0, 0^0 and -10^0. The numerical and experimental results are presented for both straight and contoured end-wall of high-pressure turbine stator cascade.

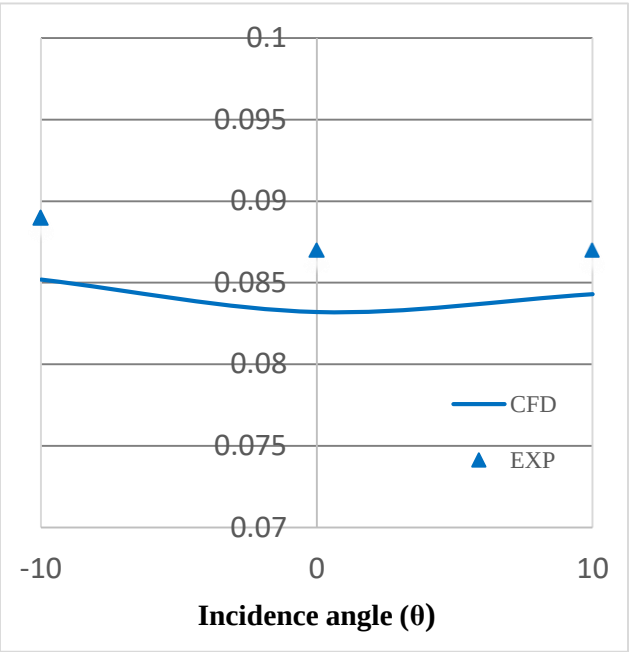

For straight end-wall

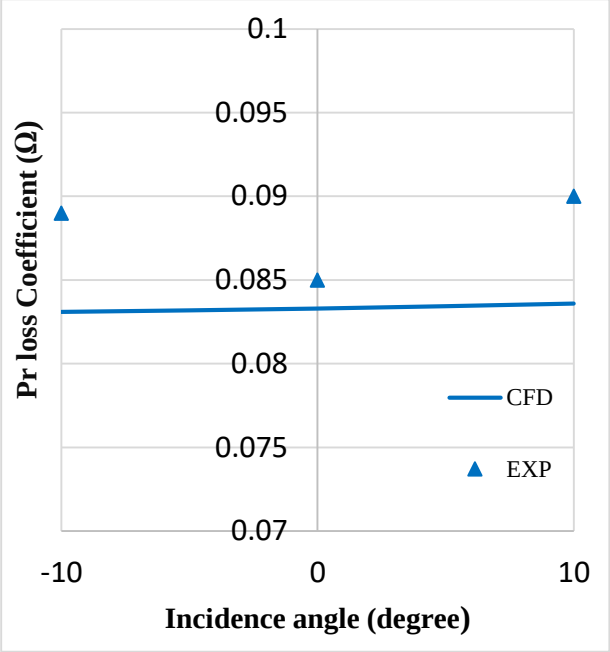

For Contoured end-wall

Fig. 9 Effect of incidence on the pressure loss coefficient at M_2-0.98.

D. Pressure Loss Coefficient at Different Outlet Mach Number

In the below figure 13 shows how coefficient of pressure loss is varying at different exit Mach number for straight and contoured end wall cases. The pressure loss coefficient in contoured end wall shows less as compared than straight end wall. So, contoured end wall can decrease the pressure losses marginally.

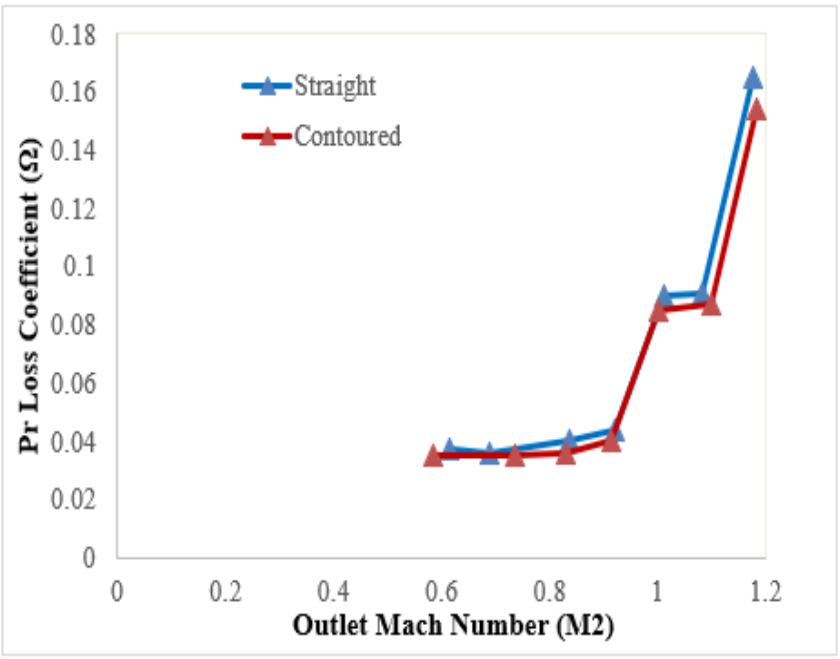

Fig. 10 Outlet Mach number on pressure loss coefficient at design incidence.

E. Mach number contours at design incidence

For both straight and contoured end-wall the Mach number contours are representing the how Mach number is distributed on the symmetry in of the computational domain for 0.98 Mach numbers design incidence (β_1 - 0^0). We can observe that the plots are showing exact outlet Mach number at the trailing edge as shown in the below figures.

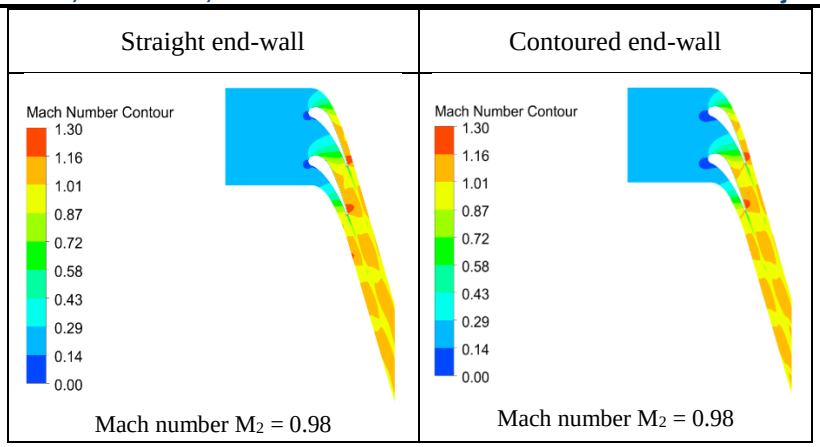

Fig. 11 Mach number contours at β_1 - 0^0, for designed Mach numbers.

F. Mach Number Contours at Design Mach Number for Different Incidence

The figure 12 shows that, how Mach number is distributed on the symmetry at an incidence of 0^0, 10^0 and -10^0 for design Mach number.

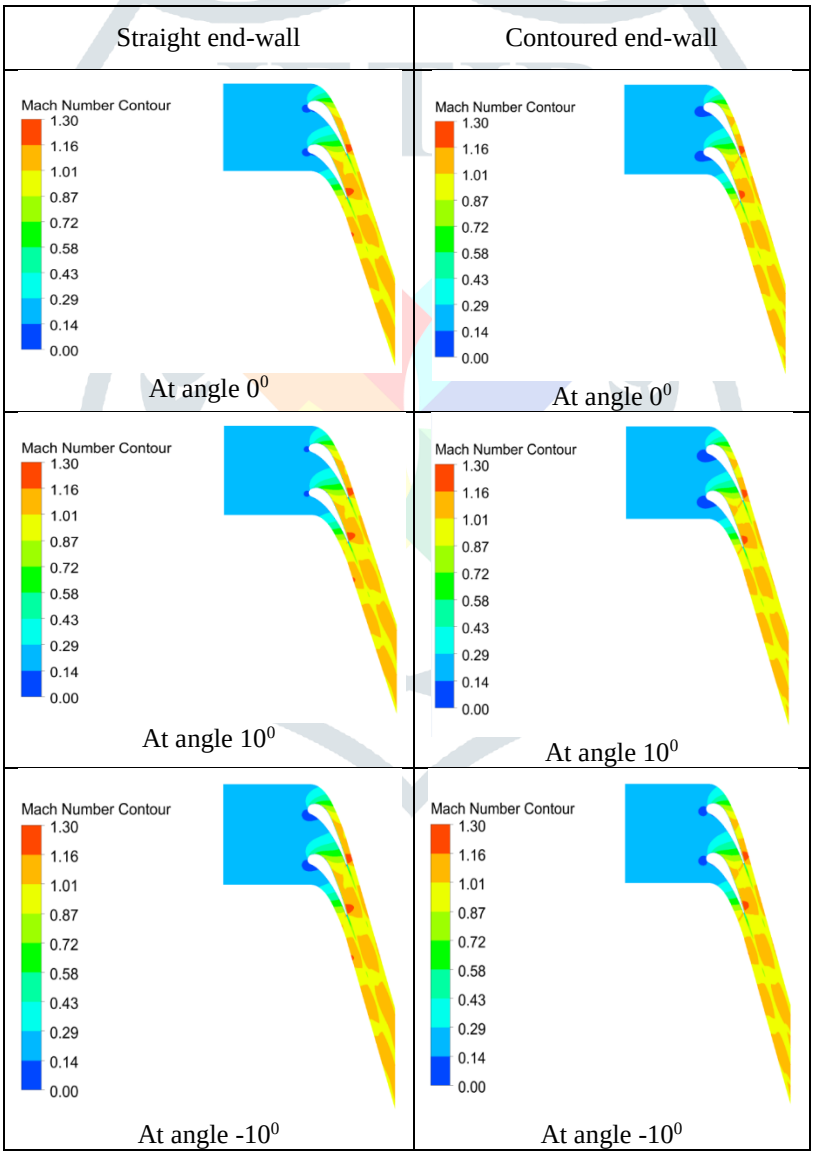

Fig. 12 Mach number contours at different angle of incidence, for Mach number M_2-0.98.

G. Oil Flow Visualization

Oil flow visualization was considered for the desired condition of β_1-0 and M_2-0.98 with the straight and contoured end-walls cascade. The pressure and suction surfaces with oil flow pattern are in below figures.

Streamlines on the blade surfaces show that the flow pattern was very clean without any separations. A narrow secondary flow zone spread between 0 to 15% of span can be noticed near the end-wall.

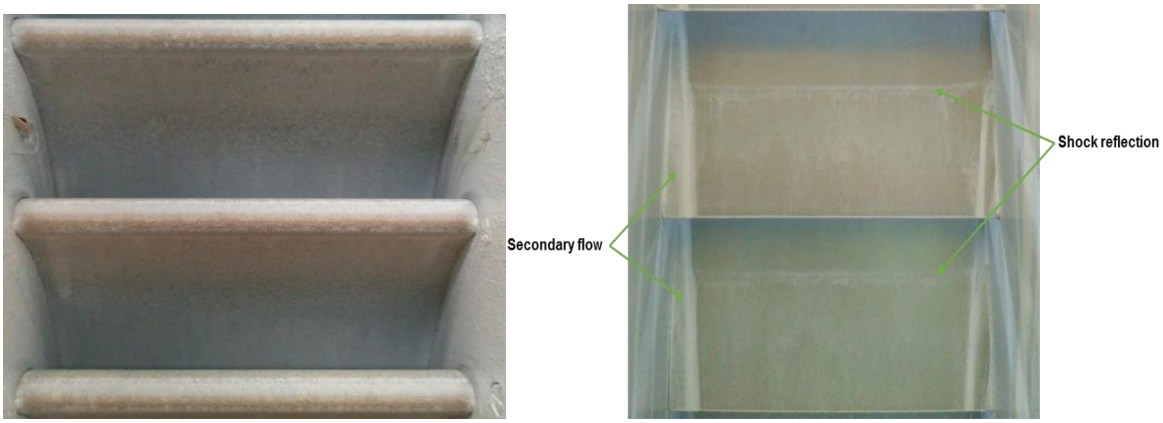

Fig. 13 Oil flow pattern on pressure and suction surface of the cascade with straight end-wall.

V. CONCLUSIONS

The turbine stator cascade was investigated with straight and contoured end walls. Numerical simulations were implemented by make use of Reynolds-averaged Navier–Stokes based solver and Shear stress transport turbulence model. Experiments were carried out by cascade testing over a range of flow conditions. Both the straight and contoured end wall configurations exhibit similar loss trends at mid span as shown in fig. 11 However, contoured end-wall configuration shows fractionally lower loss due to higher Axial Velocity Density Ratio [1] and tested for all type of outlet Mach numbers. Loss coefficient is measured to be around 9% at straight and 8.5% at contoured end wall for the design outlet Mach number (M_2-0.98). The profile remained insensitive over the tested range of incidence angles. Tests with contoured end wall showed a reduction in peak Mach number from 1.4 to 1.2 as compared with straight end wall at design condition. As a result, the losses also decrease due to the drop-in shock strength. Very clean flow pattern was observed on the cascade blade surfaces without any separations with both the end wall cases. A narrow secondary flow zone spread between 0 to 15% of span was noticed near the contoured end-wall. This shows that there is less losses at the contoured end wall.

VI. ACKNOWLEDGEMENTS

The authors thank to director of CSIR-NAL, for permitting to carry out this work and for allowing it to be publish. Authors are grateful to Department of mechanical engineering, SIT for their encouragement. Authors express sincere gratitude to the other members for their support while doing this work

REFERENCES

[1] J P Gastelow, "*Cascade Aerodynamics*", Pergamon Press. First edition, 1984

[2] Rolls-Royce plc Derby England "*The jet engine*" Fifth edition, 1996.

[3] E de la Rosa Blanco, H P Hodson, R Vazquez and D Torre Influence of the state of the inlet endwall boundary layer on the interaction between pressure surface separation and endwall Flows Instn Mech. Engrs Vol. 217, 2003.

[4] Neil W. Harvey, Martin G. Rose, Mark D. Taylor, "*Non-axisymmetric Turbine End Wall Design: Part I-Three-Dimensional Linear Design System*" ASME Vol. 122, APRIL 2000

[5] G Ingram, D Gregory-Smith and N Harvey, "*The benefits of turbine endwall profiling in a cascade*" IMechE Vol. 219, 2005

[6] M. Govardhan and P. K. Maharia, "*Improvement of Turbine Performance By Streamwise Boundary Layer Fences"* Journal of Applied Fluid Mechanics, Vol. 5, No. 3, pp. 113-118, 2012.

[7] Rose M., Harvey N., Seaman P., Newman D., McManus D.: Improving the Efficiency of the Trent 500 HP Turbine Using Non-Axisymmetric End Walls. Part II: Experimental Validation, ASME-Paper 2001-GT-0505, (2001).

[8] Sieverding C. H., 1985, ''*Secondary flows in straight and annular turbine cascades*" Ucer, Stow, and Hirsch, eds., Thermodynamics & Fluids of Turbomachinery, NATO, Vol. II, pp. 621–624.

[9] Hartland J. C., Gregory-Smith D. G., and Rose M. G., 1998, ''*Non-Axisymmetric End-wall Profiling in a Turbine Rotor Blade*'' ASME Paper No.98-GT-525.

[10] Bardia J. E., Haung P.G., Caukely T.J., "Turbulence Modeling, Validation, Testing and Development", NASA Technical Memorandum 110446, 1997.
[11] Mentor F. R., "Zonal two equation κ-ω turbulence models for aerodynamic flows" AIAA paper, 93-2906, 1993.
[12] Pankhurst R.C. and Bryer D. W., "Pressure-probe methods for determining wind speed and flow direction", National Physical Laboratory, London, ISBN 0 11 480012 X.
[13] Private conversations with Mr.R.Senthil Kumaran, Principal Scientists, PR Division NAL.